Structural Model for Longitudinal Cracking in Bonded Whitetopping with a 1.83-m x 1.83-m (6-ft x 6-ft) Joint Spacing

Zichang Li[1], Julie M. Vandenbossche[2], M. ASCE. P.E., and Nicole Dufalla[3], S.M.ASCE

1 Graduate Student Researcher, Department of Civil and Environmental Engineering, University of Pittsburgh, 713 Benedum Hall, 3700 O'Hara Street, Pittsburgh, PA 15261. Email: zil4@pitt.edu

2 Assistant Professor, Department of Civil and Environmental Engineering, University of Pittsburgh, 705 Benedum Hall, 3700 O'Hara Street, Pittsburgh, PA 15261 (Corresponding author). Email: jmv7@pitt.edu

3 Graduate Student Researcher, Department of Civil and Environmental Engineering, University of Pittsburgh, 713 Benedum Hall, 3700 O'Hara Street, Pittsburgh, PA 15261. Email: nid27@pitt.edu

Abstract: Longitudinal cracking has been identified as the predominant distress in thin bonded whitetopping with a 1.83-m (6-ft) longitudinal joint spacing. However, the structural models in existing whitetopping design procedures do not address this particular mode of failure. To better predict the design stresses and therefore to provide a more accurate design, a new structural model for predicting longitudinal cracking, which accounts for the combined effect of wheel load and temperature gradient, was developed using one specific three-dimensional finite-element model. The model was validated by matching field deflection data from existing whitetopping sections to predicted deflections. A database was populated with this model and was used in the development of a new closed form structural model to predict the critical stress with respect to longitudinal cracking. A sensitivity study was conducted to evaluate the new structural model. (Word count: 134)

CE Database subject headings: Concrete pavements, pavement overlays, structural models, structural failures, finite element method

Author Keywords: whitetopping, structural model, longitudinal cracking, finite element model

Number of figures: 7
Number of tables: 4
Word count: 4,110

1. INTRODUCTION

Bonded whitetopping is a rehabilitation procedure consisting of placing a relatively thin Portland cement concrete (PCC) overlay on a deteriorated hot-mixed asphalt (HMA) pavement. This technique has gained popularity since the 1990s and, as a result, much effort has been put towards the development of design procedures (Rasmussen and Rozycki 2004, Rasmussen et al 2002, Barman et al 2013), many of which were published between 1998 and 2010 (Roesler et al 2008, Wu et al 1998, Tarr et al 1998, Gucunksi 1998, ACPA, Sheehan et al 2004). The first used for designing ultra-thin whitetopping (UTW, 51-102 mm [2-4 in] thick) in the United States, was published by the Portland Cement Association (PCA) in 1994 (Wu et al 1998) and was intended for the design of lower volume roads. This procedure was later improved by the Illinois Center for Transportation (ICT) in 2008 (Roesler et al 2008), in-part by providing a means for accounting for the effect of the use of structural fibers on increased toughness. This revised procedure currently serves as the basis for the web application developed by the American Concrete Paving Association (ACPA). The design procedure available for designing thin whitetopping (TWT, greater than 102 mm [4 in] but less than 152 mm [6 in] thick), was published by the Colorado Department of Transportation (CDOT) to provide a bonded overlay alternative for heavier trafficked roadways. Revisions were made to this procedure in 2004 (Wu et al 1998, Sheehan et al 2004).

During the initial development of these procedures, little performance data existed and consequently the failure modes were developed using data from strain measurements and finite element modeling. In these procedures, the failure modes were defined based on slab thickness: corner cracking for UTW and transverse cracking for TWT. However, as more field performance data became available, it was evident that the failure mode was dictated by slab size rather than overlay thickness (Barman et al 2013, Li and Vandenbossche 2013). This implies that it is the location of the wheelpath with respect to the joint locations that defines the failure mode for whitetopping.

Longitudinal cracking was found to be the predominant distress for whitetopping with a 1.83-m x 1.83-m (6-ft x 6-ft) joint spacing (Li and Vandenbossche 2013). However, no structural model in current design guides is available for this failure mode. Additionally, the temperature considerations in the existing design procedures are largely undeveloped. The following will introduce a new structural model for estimating the critical stress when predicting the development of longitudinal cracking. A sensitivity study will also be presented that will show the structural model developed provides reasonable predictions for longitudinal cracking.

2. LITERATURE REVIEW

2.1 Failure modes

Investigating the failure modes in whitetopping is a relatively new area of interest, with the first comprehensive discussion being published in 2002 (Rasmussen et al 2002). UTW slabs were loaded using accelerated load testing (ALT) equipment and observed failure modes included mid-slab transverse cracking, mid-slab longitudinal cracking, corner cracking, joint faulting, and spalling. Despite these observations, no single predominant failure mode could be identified. More ALT testing followed with the University of Florida conducting ALT on a UTW section in 2007 (Gutierrez 2007). FWD testing was performed and strain measurements were taken on the section and a finite element model was developed to analyze this data. In 2008, another ALT was conducted on a UTW section at Purdue University to evaluate factors affecting the interface bond (Newbolds and Olek 2008). In 2009, ALT with unidirectional loading was conducted on whitetopping sections at the University of Illinois (Roesler et al 2012). Longitudinal cracking in the wheel path was the predominant distress observed for UTW section fatigued. The results do not incorporate environmental effects as it was loaded within a short period. It was found, however, that failure modes differed from sections over a granular base.

Since the 1990s, several whitetopping sections subjected to live traffic have been constructed in the United States (Cackler 2012, ACPA 1998). Among them, performance data from the Minnesota Department of Transportation research facility (MnROAD) was the most comprehensive (MnDOT 2009). An analysis of the data collected was compiled and reported by Vandenbossche and Fagerness (2002) with a summary of the performance of the sections summarized by (Barman et al 2013). Further investigation of whitetopping performance data indicated that failure modes were dictated by slab size rather than overlay thickness, the failure mechanism was identified to be longitudinal cracking in whitetopping with a 1.83-m (6-ft) longitudinal joint spacing but not corner or transverse cracking (Li and Vandenbossche 2013). The whitetopping sections with a 1.83-m (6-ft) longitudinal joint spacing in Colorado, Virginia, Mississippi, Illinois and Oklahoma, also predominantly experienced longitudinal cracking (Barman et al 2013)

2.2 Whitetopping Design Procedures

The two most widely used pavement design guides, the AASHTO 1993 (1993) and the MEPDG (ARA 2004) both are commonly used for designing standard PCC overlays; however, both contain limitations for the design of bonded whitetopping overlays. These limitations include the assumption of either a fully bonded or fully unbonded interface between the PCC overlay and the HMA layer, the simplification of treating the HMA layer as a stabilized base and the inability to account for slab sizes that that are less than the full lane width.

2.2.1 Corner cracking

In 1994, the PCA developed the first ultra-thin whitetopping design that accounted for the smaller slab size that is commonly adopted when constructing UTW. The limited amount of field data available revealed corner cracking to be the predominant failure mode for these slabs. The location of the critical stress was determined to be on the top of the PCC overlay for a corner loading condition and in the presence of a negative temperature gradient. This initial whitetopping procedure is the foundation of the current ACPA whitetopping design application (Wu et al 1998) and utilizes Equations 1 and 2 for stress calculations. Equation 1 gives the stress-prediction equation from the ACPA application and Equation 2 gives the temperature curling stress.

$$\sigma_{18} = 10^{5.025-0.465\log(k)+0.686\log(L/\ell_e)-1.291\log(\ell_e)} \quad (1)$$

The temperature curling stress is

$$\sigma_T = 28.037 - 3.496(CTE \times \Delta T) - 18.382(L/\ell_e) \quad (2)$$

Where,

k = modulus of subgrade reaction, psi/in

L = joint spacing (assuming square slabs), in

ℓ_e = the effective radius of relative stiffness, in

CTE = coefficient of thermal expansion, 10^{-6} in/°F/in

ΔT = the slab's temperature differential, °F.

Note that these stresses were determined using a 2-D finite element analysis and a 36 percent stress increase factor based on strain measurements from existing whitetopping sections. This is to account for partial bonding at the PCC-HMA layer interface (Roesler et al 2008).

2.2.2 Transverse cracking

In 1998, the CDOT developed a procedure for designing TWT, which typical have a thickness between 102 mm (4 in) and 152 mm (6 in) and utilizes larger slabs (e.g. 1.83 m x 1.83 m [6 ft x 6 ft]). This procedure was later revised in 2004. The failure mode was assumed to be transverse cracking with the critical load location centered along the longitudinal free edge joint and produced a critical stress at the bottom of the PCC overlay. Equation 3 gives the stress prediction

equation from the 2004 CDOT design procedure (Sheehan et al 2004) and Equation 4 gives the temperature curling stress.

$$\sigma_{18} = \frac{18}{20}\left[18.879 + 2.918\left(\frac{h_{PCC}}{h_{ac}}\right) + \frac{425.44}{\ell_e} - 6.955\times10^{-6}E_{ac} - 9.0366\log(k) + 0.0133L\right]^2 \quad (3)$$

$$\sigma_T = (3.85\times TG)\%\times\sigma_{18} \quad (4)$$

Where,

k = modulus of subgrade reaction, psi/in

L = joint spacing (assuming square slabs), in

ℓ_e = the effective radius of relative stiffness, in

TG = the slab's temperature gradient, °F/in.

The design stresses is determined by applying a 1.51 adjustment factor to account for partial bonding at the interface of the PCC-HMA layer. This was performed to calibrate the model based on strain data on a limited number of whitetopping sections constructed in Colorado. These procedures have served the pavement community well for many years. However, the whitetopping sections with a 1.83 m (6-ft) longitudinal joint spacing in Minneapolis, Colorado, Virginia, Mississippi, Illinois and Oklahoma all experienced longitudinal cracking as predominant distresses, regardless of whitetopping thickness (Barman et al 2013). Also, when considering lateral traffic distributions, the maximum consumption of the fatigue life actually occurs at the intersection of the wheel path and the transverse joint, which develops into a longitudinal crack. Therefore, the following will describe the approach taken in the development of a new structural model for estimating the critical stress when predicting the development of longitudinal cracking.

3-D FE MODEL

3.1 Six-slab Model

First, a specific 3-D finite element model was developed in this study using the general purpose finite element software ABAQUS code (ABAQUS 2004). As shown in **FIGURE 1**, the model consisted of six square slabs with a 6-ft joint spacing separated by longitudinal and transverse joints and a 5-ft wide HMA shoulder.

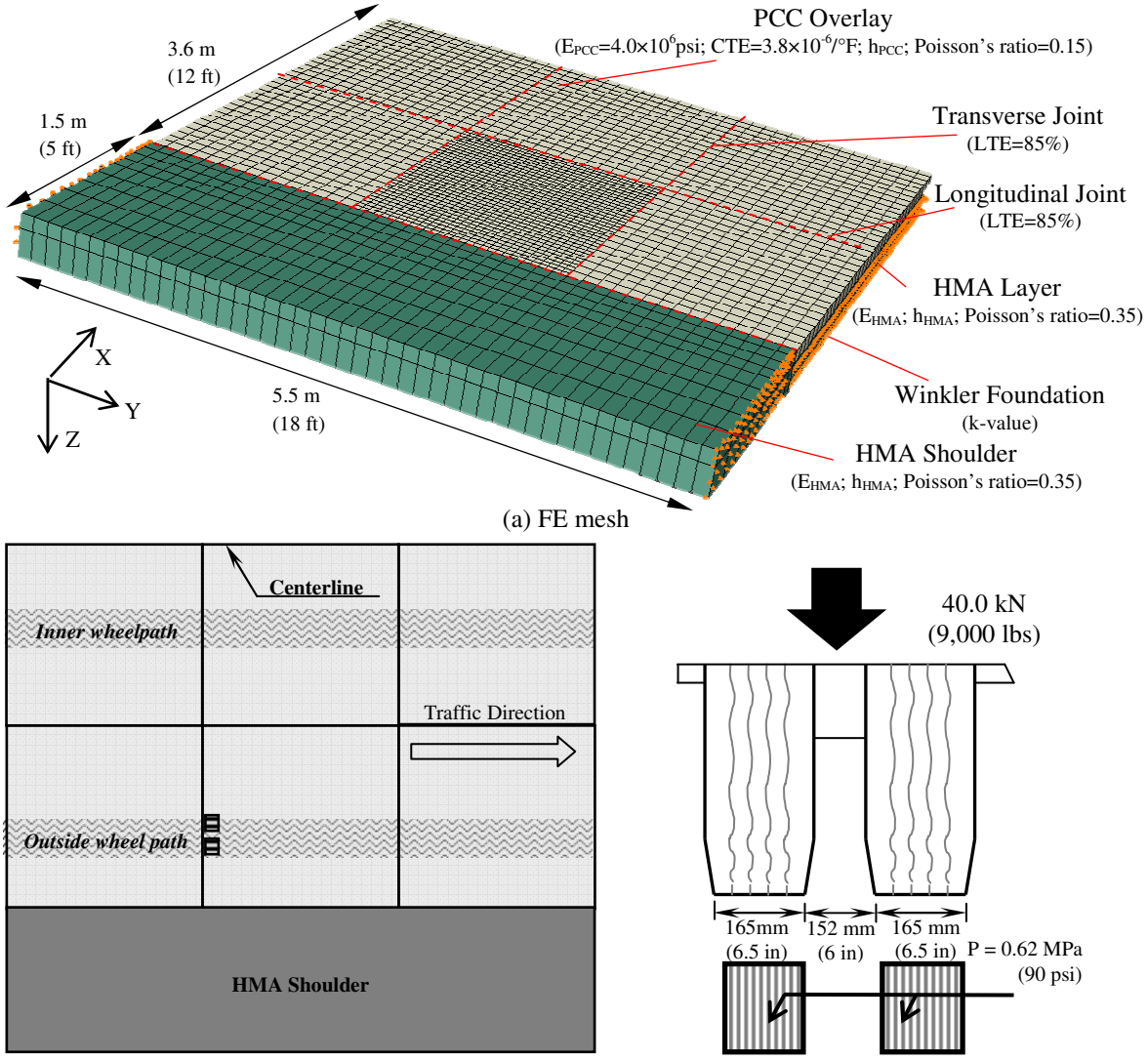

FIGURE 1. Six-slab 3-D finite element model.

Twenty-seven-node brick isoparametric elements (C3D27) were selected to model the PCC and HMA layers. This type of node configuration has been shown to provide a high level of accuracy in combination with an acceptable computational time demand (Kuo 1994).

Load transfer was considered by assigning translational springs in both transverse and longitudinal joints. Three spring constants were used to represent the stiffness at different positions, namely K_v at the corner, $2K_v$ at the edge and $4K_v$ at the inner nodes, respectively. To establish the spring constant, first a typical load transfer efficiency (ratio of the deflection on the unloaded side to the loaded side multiplied by 100%) (LTE) value of 85% from aggregate interlock was used. The spring stiffness was defined such that a combined deflection LTE, considering both asphalt and concrete pavement components, was a function of the structural features and varied between 88% and 95%. To simplify the model, "Hard Contact" property was assigned to the two surfaces at joints to take into account the compression effect.

The PCC-HMA interface is critical to the performance of bonded whitetopping. Preliminary studies indicated that the interface bond only affected the service life of whitetopping with a 6-ft joint spacing but did not change the predominant failure mode (Nishiyama et al 2003).

To develop a new structural model, a fully-bonded interface was simulated by employing the "TIE" connectors at the PCC-HMA interface. While partial bonding has yet to be fully understood, a fully bonded interface is modeled, which will allow for future adjustment to incorporate partial interface bonding.

This model was first used to identify the critical failure mode in whitetopping with a 1.83-m x1.83-m (6-ft x 6-ft) joint spacing in previous research (Li and Vandenbossche 2013). With longitudinal cracking identified as the predominant distress in whitetopping with a 1.83-m x1.83-m (6-ft x 6-ft) longitudinal joint spacing, the corresponding critical loading scenario is in the wheelpath directly adjacent to the transverse joint.

3.2 Convergence Check

Two models with different mesh fineness were run to ensure convergence of the stress and displacement. The stress contours are comparable and have identical critical stress locations. As shown in **TABLE 1**, the proposed model achieves adequate accuracy with a stress tolerance of 5.0%. Also, Kuo (1994) showed that using higher-order elements only requires one element along the thickness of each layer to obtain accurate stress calculations at the top and bottom of the PCC slab.

TABLE 1. Mesh convergence by size, mm (in).

	Mesh size, mm × mm × mm (in × in × in)	
	102 × 102 × 102 (4 × 4 × 4)	51 × 51 × 51 (2 × 2 × 2)
Critical stress on top of PCC overlay, MPa (psi)	0.605 (87.8)	0.603 (87.4)
Critical stress at bottom of PCC overlay, MPa (psi)	1.409 (204.4)	1.473 (213.7)
Maximum deflection, mm (mil)	0.2728 (10.74)	0.2736 (10.77)

3.3 Validation with Field Measurement

In order to accurately analyze the behavior of whitetopping using the 3-D analytical model, two whitetopping sections, Cells 62 and 60 at MnROAD, were used for validating the model. Additional design features for Cells 62 and 60 can be found in the references (Barman et al 2011) and (Li and Vandenbossche 2013) but are briefly summarize in **TABLE 2**.

TABLE 2. Pavement parameters in Cells 60 and 62 (Burnham 2006, Vandenbossche and Fagerness 2002).

Parameter	Cell 62	Cell 60
HMA thickness, mm (in)	203 (8.0)	178 (7.0)
HMA modulus of elasticity, GPa (10^6psi)	2.4 (0.35)	2.4 (0.35)
PCC thickness, mm (in)	102 (4.0)	127 (5.0)
PCC Poisson ratio	0.13	0.18
PCC modulus of elasticity, GPa (10^6psi)	33.8 (4.9)	31.7 (4.6)
Modulus of subgrade reaction, kPa/mm, (psi/in)	85.5 (315)	85.5 (315)
CTE, 10^{-6}/°C (10^{-6}in/°F/in)	6.84 (3.8)	7.38 (4.1)
K_v*, N/mm (lbs/in)		244 (1,392)
K_t, K_n, N/mm (lbs/in)		1,751 (10,000)

* Previous work (Li and Vandenbossche 2013) indicated that the effect of LTE on stress is negligible in fully-bonded whitetopping.

FIGURE 2 shows the predicted and measured deflection basins resulting from 40- and 67-kN (9- and 15-kip) FWD loads applied to the center, transverse joint, mid-edge and corner of the slabs, respectively, in Cell 62. It is clear that the computed FWD deflections match well with the measured deflections for a fully bonded HMA-PCC interface.

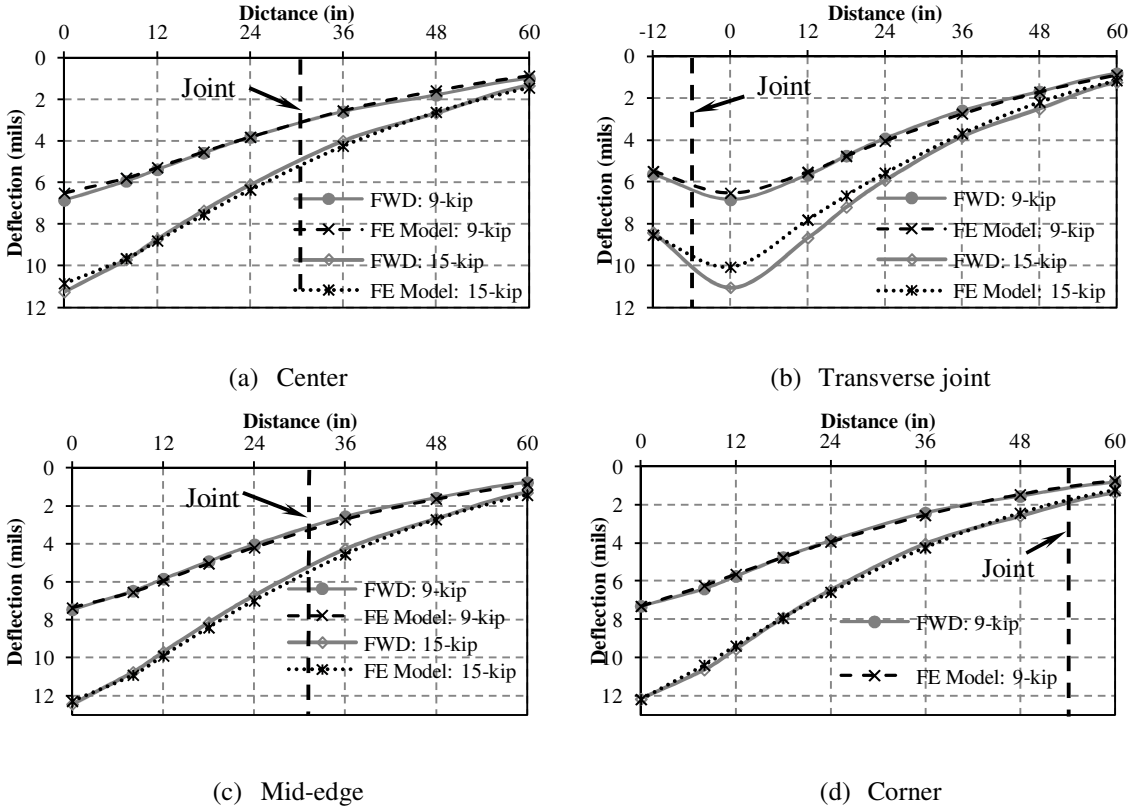

(a) Center (b) Transverse joint

(c) Mid-edge (d) Corner

FIGURE 2. Matching of deflection basins for 9- and 14-kip FWD in Cell 62.

The results for Cell 60 are shown in **FIGURE 3**. Unlike Cell 62, the computed FWD deflections matched better with the measured deflections when the PCC-HMA interface was modeled as partially bonded. Rather than tying node connections as was done for the fully bonded model, transverse spring connections were used in both the x and y directions to simulate partial bonding. Details on the development of the model for the partial bond can be found in (Li and Vandenbossche 2013)

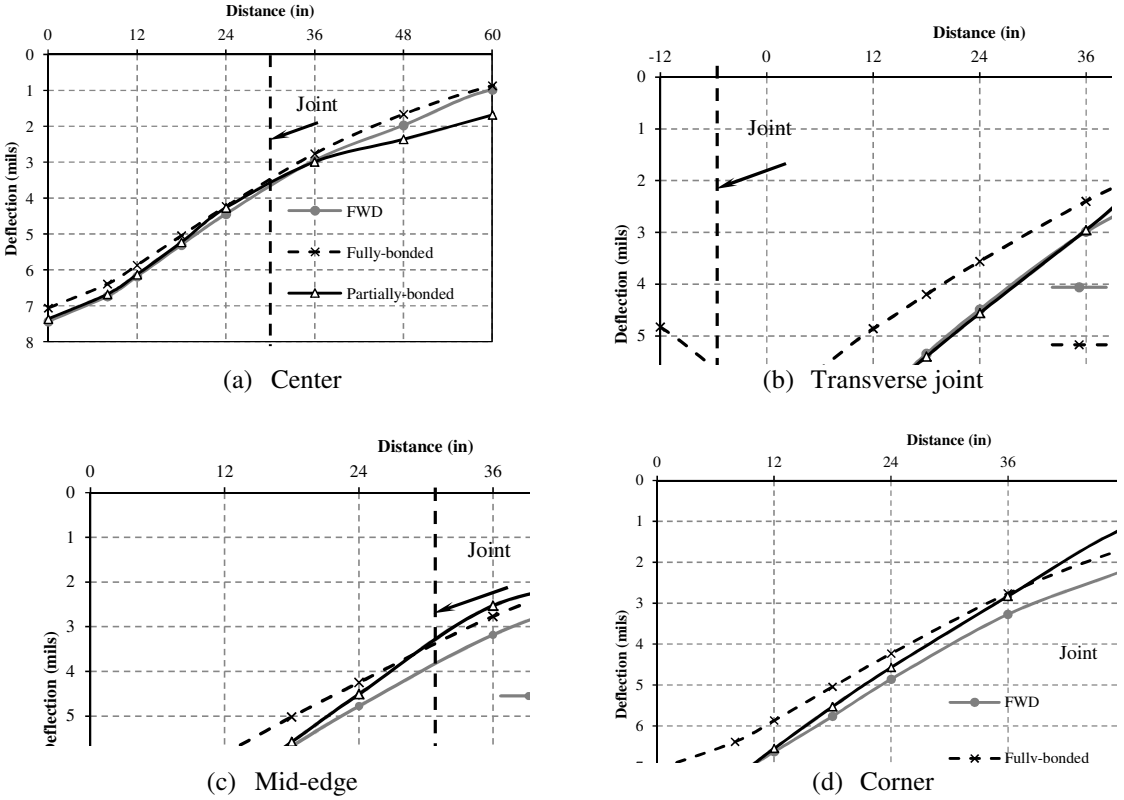

FIGURE 3. Matching of deflection basins caused by 40-kN (9-kip) FWD in Cell 60.

3.4 Wheel Load Configurations

As presented in reference (Li and Vandenbossche 2013) the critical loading condition in whitetopping with a 1.83-m x 1.83-m (6-ft x 6-ft) joint spacing is in the wheelpath adjacent to the transverse joint, as shown in **FIGURE 3** (b). The slabs were loaded with a 40-kN (9-kip) single-axle dual-wheel load with a tire pressure of 0.62 MPa (90 psi). The load area was assumed to be rectangular with an evenly distributed load, as shown in **FIGURE 3** (c). Because the model was discrete and the pressure load in the ABAQUS program has to be applied on the element faces, the final contact area was adjusted according to the geometry of the elements. Equivalent areas and pressure were used for the contact area but the simplified geometry led to a different actual contact shape.

3.5 Temperature Gradients

FEM runs indicated that the temperature-induced stresses were considerably smaller than the wheel load-induced stresses. This was confirmed by the field investigation performed by CDOT when the temperature restraint stresses were collected while load testing but were not ultimately included in the CDOT design procedure developed in 1998 (Greene et al 2009). However, the effect of the temperature-induced stress is not negligible. Temperature-induced stresses alone are typically low; however, the stresses substantially increase when compounded with wheel loading. The initial study showed that because of the relative thinness of the PCC overlay, the continuity of the HMA layer, and the inherent variable stiffness of the HMA, the corner loading stress at the top of the PCC overlay is considerably smaller than the stress at the bottom of the PCC overlay (Li and Vandenbossche 2013). Thus, the temperature-induced stresses under with the wheel load applied adjacent to the transverse joint in the wheelpath were investigated.

The concrete slab temperature was assumed to vary linearly from the top to the bottom of the overlay, where the bottom of the overlay was assumed to remain the same as the initial temperature. Two temperature gradients, 0.328°C/cm and 0.656°C/cm (1.5°F/in and 3.0°F/in), were chosen as typical values and were investigated under 40 kN (9-kip) wheel loads to evaluate the effect of the gradient magnitude. The total number of FEM iterations was 2,304 for temperature consideration. The inclusion of a third point, the case of a zero-stress gradient, allowed for investigation of the nonlinear behavior of temperature-induced stress.

3.6 Experimental design

For the wheelpath loading condition, the following combinations of parameters were investigated. The inference space used for the wheelpath loading condition is given in **TABLE 3** utilizing a range of typical values used in a total of 2,880 FEM runs. These iterations include the typical ranges for PCC overlay thickness, HMA layer thickness, modulus of subgrade reaction, and HMA modulus.

TABLE 3. Parameter ranges investigated in FEM runs.

Parameter	Values
HMA thickness, mm (in)	76.2, 127.0, 177.8, 228.6 (3, 5, 7, 9)
PCC thickness, mm (in)	76.2, 101.6, 127.0, 152.4 (3, 4, 5, 6)
Modulus of subgrade reaction, kPa/mm (psi/in)	13.6, 40.7, 81.3, 135.5 (50, 150, 300, 500)
HMA modulus of elasticity, GPa (10^6 psi)	1.38, 2.76, 4.14, 5.52, 6.89, 10.34, 13.79, 20.68, 27.58 (0.2, 0.4, 0.6, 0.8, 1.0, 1.5, 2.0, 3.0, 4.0)
PCC modulus of elasticity, GPa (10^6 psi)	27.58 (4.0)
Joint spacing, m (ft)	1.83 (6.0)
LTE, %	85.0
PCC Poisson's ratio	0.15
HMA Poisson's ratio	0.35
CTE, cm/°C/cm (in/°F/in)	6.8×10^{-6}, 9.9×10^{-6} (3.8×10^{-6}, 5.5×10^{-6})
Temperature gradient, °C/cm (°F/in)	0, 0.328, 0.656 (0.0, 1.5, 3.0)

4 RESULTS AND ANALYSIS

4.1 Stress prediction equation development

The stress prediction equation was derived using multiple predictors, and is presented in Equation 5. A total of 576 cases with zero temperature gradient were run. To be conservative, the stresses were considered to be zero if they were negative (in compression).

$$\sigma_{Wheel} = e^{\frac{\left(89.4014+0.0512h_{HMA}^2+8.6096h_{PCC}\right)-\log(NA)\left[27.4911+7.7478h_{PCC}+7.7478\log(kE_{HMA})\right]}{15}}+10 \quad (5)$$

Where,

σ_{Wheel} = maximum stress in the PCC overlay under 18-kip wheel load, psi
h_{HMA} = thickness of the HMA layer, in
h_{PCC} = thickness of PCC overlay, in
E_{HMA} = HMA modulus of elasticity, psi

k = modulus of subgrade reaction, psi/in
NA = neutral axis from top of PCC overlay, in, which is given in Equation 6.

$$NA = \left[\frac{E_{PCC} h_{PCC}^2}{2} + E_{HMA} h_{HMA} \left(h_{PCC} + \frac{h_{HMA}}{2} \right) \right] \Big/ \left(E_{PCC} h_{PCC} + E_{HMA} h_{HMA} \right) \quad (6)$$

FIGURE 4 compares the predicted versus calculated results from the stress-prediction equation and the FEM runs, respectively. As shown in the figure, the overall prediction is good with an R-square of 0.96.

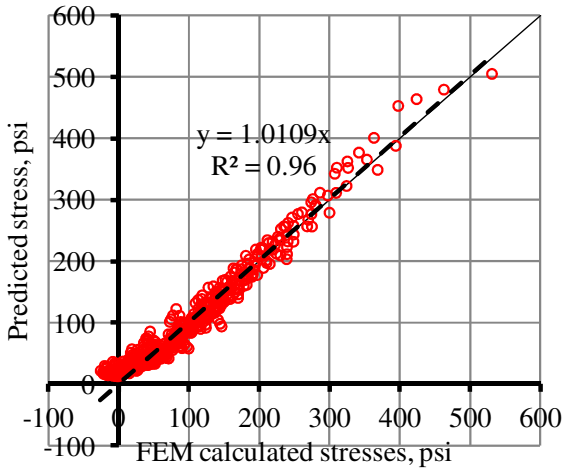

FIGURE 4. Predicted vs. FEM calculated critical stresses at the bottom of PCC overlay.

The temperature-induced stress under the wheel-load effect is obtained from combining the wheel load and temperature-induced stresses and subtracting the stresses from the wheel load alone. Equation 7 presents this concept. The total number of FEM runs for this stress calculation was 2,304 including a zero-temperature-induced-stress case where slab curling and warping are absent. **FIGURE 5** shows the overall prediction versus calculated stress for this estimate, and, as shown, a good prediction is achieved with an R-square of 0.92.

$$\Delta\sigma_{TG} = CTE^{1.07} \times TG \times (0.0278 \times TG + 0.3334) h_{PCC}^{[0.195812 \log(h_{HMA}) + 1.45028]} \quad (7)$$

Where,

$\Delta\sigma_{TG}$ = stress induced by temperature gradient in PCC overlay, psi
CTE = slab's coefficient of thermal expansion, 10^{-6} in/°F/in
TG = temperature gradient in PCC overlay, °F/in.

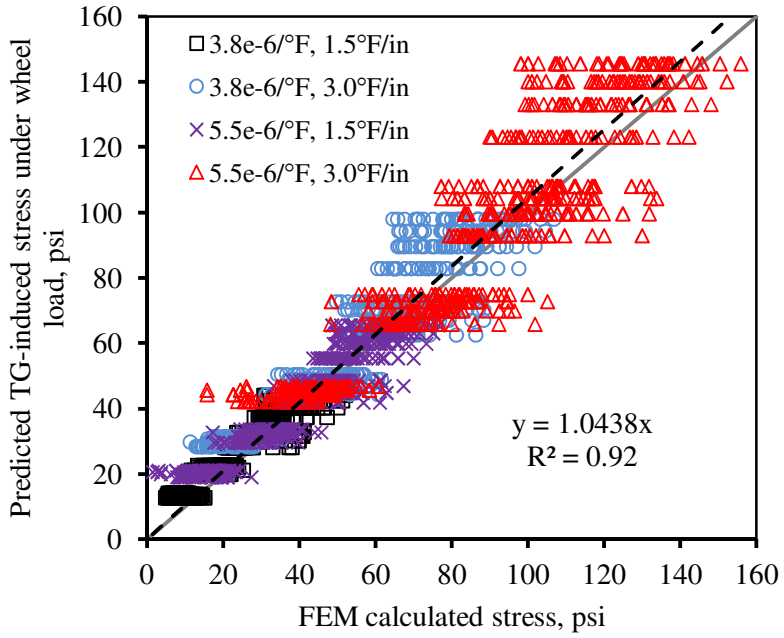

FIGURE 5. Predicted vs. FEM calculated temperature under wheel loads.

5 SENSITIVITY ANALYSIS

In order to evaluate the new structural model, a sensitivity analysis of the design inputs on the predicted stresses was performed. For this, an inference space was established for each input and these values are summarized in **TABLE 4**.

TABLE 4. Summary of standard input values used in sensitivity analysis.

Variables	Standard Input	Sensitivity Range
PCC thickness, mm (in)	101.6 (4.0)	63.5 - 152.4 (2.5 - 6.0)
CTE, 10^{-6} cm/°C/cm (10^{-6} in/°F/in)	9.9 (5.5)	6.8, 8.1, 9.9, 13.5 (3.8, 4.5, 5.5,7.5)
HMA thickness, mm (in)	152.4 (6.0)	50.8 - 254.0 (2.0 - 10.0)
Modulus of subgrade reaction, kPa/mm (psi/in)	54.2 (200)	13.6 - 108.4 (50 - 400)
HMA modulus of elasticity, GPa (10^6 psi)	2.07 (0.3)	0.69 - 2.76 (0.1 - 4.0)
Temperature gradient, cm/°C/cm (in/°F/in)	5.4 (3.0)	0.0 - 7.2 (0.0 - 4.0)
Joint spacing, mm (in)	1,830 (72)	

5.1 Predicted Stress due to Wheel Load

FIGURE 6 shows the predicted stress due to the wheel load calculated using Equation 5 as a function of HMA elastic modulus, HMA thickness, PCC elastic modulus and subgrade reaction, respectively. The revised model, as presented in Equation 5, was plotted in **FIGURE 6** to illustrate the trends of the new structural equation.

Shown in **FIGURE 6**(a), **FIGURE 6**(b) and **FIGURE 6**(d), the critical stresses calculated by both models exhibit high sensitivity to the HMA modulus. It is important to note that the locations of these critical stresses differ because of the geometrical configuration of the slab. Therefore, the maximum critical stresses are compared despite occurring in different locations. The observed sensitivity to the HMA modulus has previously been discussed in references 0 and 0. Recently, the modified whitetopping design procedure 0 accounted for the temperature dependency of the HMA modulus and utilized a master curve for better prediction based on climate and other input factors.

FIGURE 6(b) indicates that the critical stresses can be reduced by increasing the thickness of HMA layer. The contribution of the HMA thickness is not proportional to itself. A thinner HMA layer has a greater effect on changing the stress. **FIGURE 6**(c) indicates that the predictions are not sensitive to the PCC elastic modulus. **FIGURE 6**(d) indicates that the critical stresses are not directly sensitive to the subgrade reaction. A better base or subgrade would decrease the critical stresses and therefore improve the performance of the whitetopping, which was validated by the accelerated load testing performed by Roesler, et al (2013).

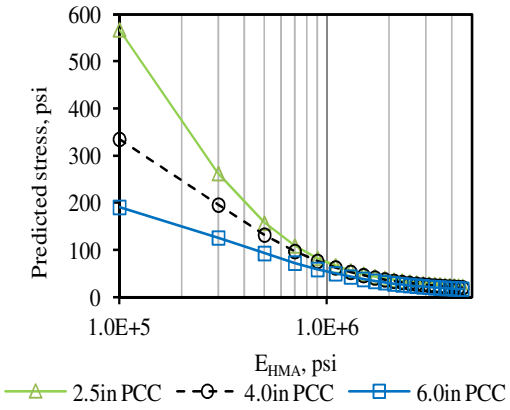

a) Elastic modulus of HMA layer

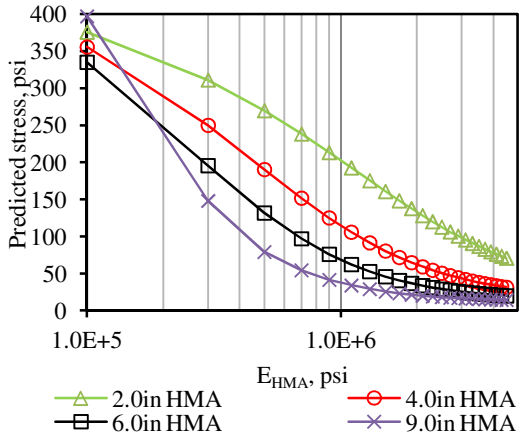

(b) Thickness of HMA layer

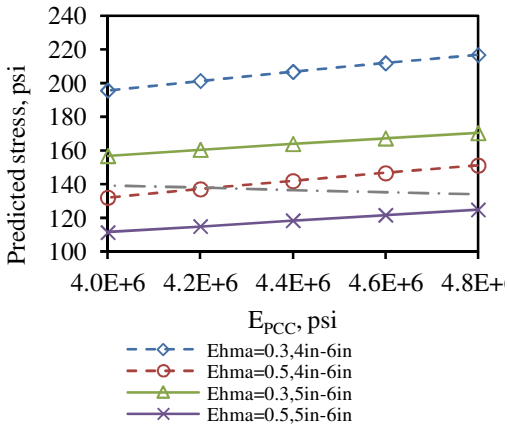

(c) Elastic modulus of PCC overlay (PCC - HMA)

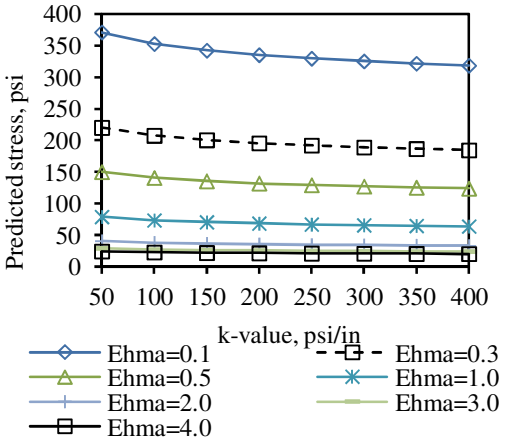

(d) Subgrade reaction

FIGURE 2. Predicted stress sensitivity study.

5.2 Temperature-induced Stress

FIGURE 7 shows the stresses induced by the temperature gradient as a function of HMA thickness, PCC thickness, temperature gradient, and slab's CTE, respectively. Results from the proposed model, as presented in Equation 7 was plotted in **FIGURE 7.**

The temperature-induced stresses are not sensitive to the HMA thickness, as shown in **FIGURE 7** (a). However, increasing the thickness, and consequently the stiffness, of the HMA layer resulted in a higher stress due to restraint of the HMA layer on the PCC overlay. **FIGURE 7** (b) shows that for the revised equation, sensitivity to temperature gradient increases with PCC thickness. **FIGURE 7** (b) and **FIGURE 7** (c) indicate a nonlinear relationship between the temperature-induced stresses from Equation 7 and the temperature gradient and the PCC thickness, respectively.

Only two CTE values, 6.8×10^{-6} and 9.9×10^{-6}/°C (3.8×10^{-6} and 5.5×10^{-6} in/°F/in), were used to populate the database for the temperature-induced stress prediction equation; therefore, an additional 24 FEM runs with varying CTE values, specifically 8.1×10^{-6} and 13.5×10^{-6}/°C ($4.5\times10^{-}$

^{6} and 7.5×10^{-6} in/°F/in), respectively, and temperature gradients, specifically 0.328, 0.656 and 0.984 °C/cm (1.5, 3.0 and 4.5 °F/in), respectively, were performed and the results were plotted versus predicted stress, as showed in **FIGURE 7** (d). The overall prediction is good with an R-square of 0.97.

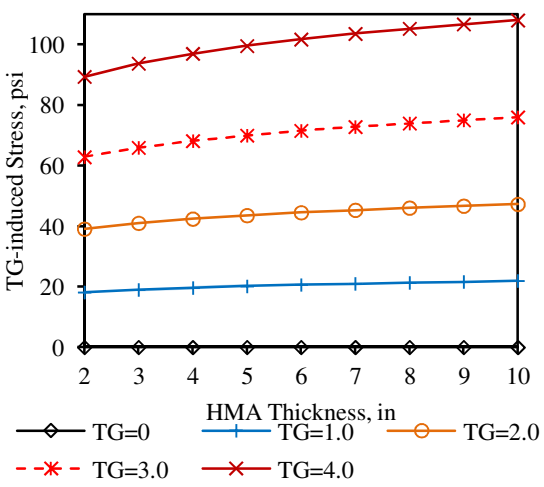

(a) Thickness of HMA layer

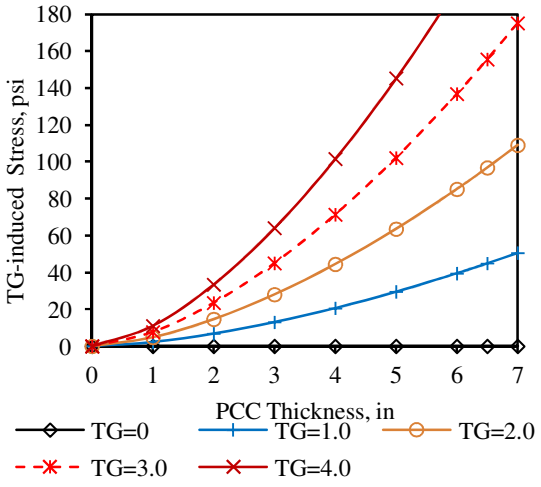

(b) Thickness of PCC overlay

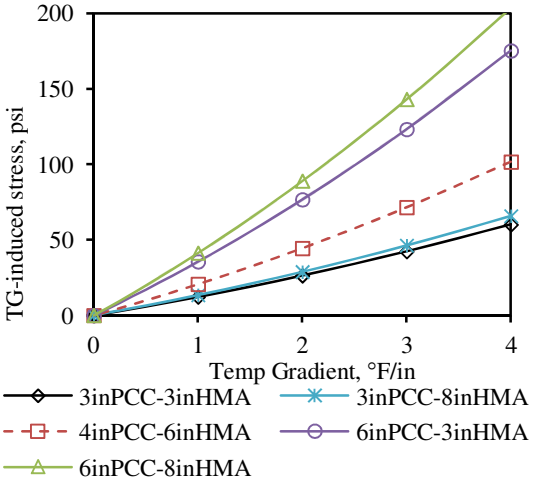

(c) Temperature gradient in PCC overlay

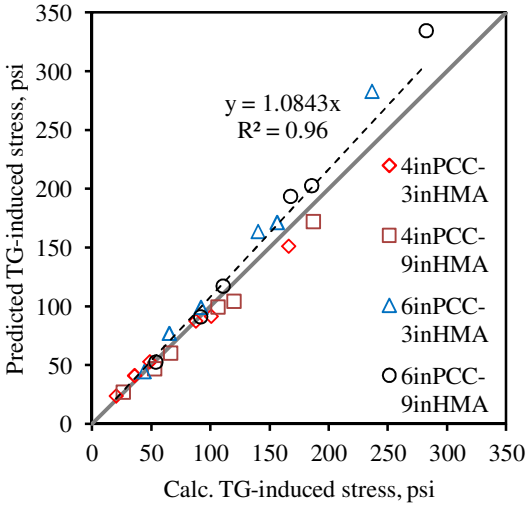

(d) CTE of PCC

FIGURE 7. Temperature-induced stress sensitivity study.

6 CONCLUSIONS

The predominant failure mode of whitetopping with a 1.83-m (6-ft) longitudinal joint spacing was recently identified to be longitudinal cracking in the wheel path (Li and Vandenbossche 2013). As no structural model is available for this type of distress in existing design procedures, a new structural model was developed in this paper to better predict the critical stresses and therefore to provide a more accurate design. The structural model consists of a stress-prediction equation and a temperature-induced stress equation. A 3-D FE model was developed in this study, which was validated by matching the deflections with the FWD data. The model was used to populate a

database generated for performing a regression analysis by using a parameter matrix covering the typical ranges of whitetopping structural features.

The proposed equations make adjustments to the CDOT and PCA structural models and adjust for temperature considerations as necessary, as they considered longitudinal cracking and combined effect of the wheel load and temperature gradient. Particular observed improvements include the new structural model is targeted for the longitudinal cracking in whitetopping with a 1.83-m (6-ft) longitudinal cracking. The new stress-prediction equation provides reasonable results when the temperature-dependent HMA stiffness is considered. Additionally, the predicted stress increased with the PCC stiffness and decreased with increasing subgrade reaction. It was also found that the new temperature stress equation indicates a nonlinear relationship of the temperature induced stress to the HMA thickness, the PCC thickness and the temperature gradient, as would be expected.

ACKNOWLEDGEMENTS

The authors would like to thank the Iowa, Kansas, Minnesota, Missouri, Mississippi, New York, North Dakota, North Carolina, Pennsylvania, and Texas Departments of Transportation. These states are all participating in the FHWA Pooled Fund Study TPF 5-165 under which this work was performed.

REFERENCES

ABAQUS (2004). *ABAQUS software version 6.5: Analysis user's manual*, Providence, R.I.

American Association of State Highway and Transportation Officials (AASHTO) (1993). *Guide for Design of Pavement Structures,* American Association of State Highway and Transportation Officials, Washington, D.C.

American Concrete Pavement Association (ACPA) Bonded Concrete Overlay on Asphalt (BCOA) Thickness Designer (http://apps.acpa.org/apps/bcoa.aspx)

American Concrete Pavement Association (ACPA) (1998). *Whitetopping—State of the Practice*, ACPA Publication EB210P, American Concrete Pavement Association, Skokie, IL.

Applied Research Associates (ARA), Inc., ERES Division. (2004). *Guide for Mechanistic-Empirical Design of New and Rehabilitated Pavement Structures*, Final Report NCHRP 1-37A, Transportation Research Board of the National Academies, Washington, D.C. www.trb.org/mepdg/guide.htm. pp. 2.4.26.

Barman, M., Vandenbossche, J.M., Mu. F., and Gatti, K. (2011). *Development of a Rational Mechanistic-Empirical Based Design Guide for Thin and Ultra-thin Whitetopping*. University of Pittsburgh. TPF 5(165)/Task 1.

Barman, M., Mu, F., and Vandenbossche, J.M. (2011). *Development of a Rational of Mechanistic-Empirical Based Design Guide for Thin and Ultra-Thin Whitetopping. Task 4 Report: Climatic Considerations*. University of Pittsburgh.

Burnham, T.R. (2006). *Construction Report for Mn/ROAD Thin Whitetopping Test Cells 60-63*. Report MN/RC -2006-18, Minnesota Department of Transportation, St. Paul, MN.

Cackler, T. (2012). "*Concrete Overlays over HMA and Composite Pavements – An Overview*," presentation at 10th International Conference on Concrete Pavements, Concrete Overlays over

HMA and Composite Pavements Workshop, Quebec City, Quebec, Canada.

Greene, J., Toros, U., Kim, T., Byron, B., and Choubane, B. (2009). *Impact of Wide-base Single Tires on Pavement Damage*. Research Report. State of Florida.

Gucunski, N. (1998) *Development of a Design Guide for Ultra-Thin Whitetopping (UTW).* Research report. NJDOT.

Gutierrez, P.E.T. (2007). *Analysis, Testing and Verification of the Behavior of Composite Pavement under Florida Conditions Using a Heavy Vehicle Simulator*. Ph.D. Dissertation, University of Florida.

Ramírez, L.C. (2010). *Concrete Mixture Properties Affecting the Aggregate Interlock Mechanism of Joints and Cracks for Rigid Pavement Systems.* Master Theses. University of Pittsburgh.

Ioannides, A.M. and Korvesis, G.T. (1990). "Aggregate Interlock: A pure-Shear Load Transfer Mechanism." *Transportation Research Record: Journal of the Transportation Research Board,* 1286. Transportation Research Board of the National Academies, Washington, D.C.

Kuo, C.M. (1994). *Three-dimensional finite element analysis of concrete pavement*. Ph.D.Dissertation, University of Illinois at Urbana-Champaign.

Li, Z., and Vandenbossche, J.M. (2013). "Redefining the Failure Mode for Thin and Ultra-thin Whitetopping with a 1.8- x 1.8-m (6- x 6-ft) Joint Spacing." *Transportation Research Record: Journal of Transportation Research Board,* Transportation Research Board of the National Academics, Washington, DC. In press.

Minnesota Department of Transportation (MnDOT)
http://www.dot.state.mn.us/Mn/ROAD/testsections/pdfs/mainline-profile-ls.pdf, Accessed February 20th, 2009.

Newbolds, S., and Olek, J. (2008). *Evaluation of Performance and Design of UltraThin Whitetopping (Bonded Concrete Resurfacing) Using Large-Scale Accelerated Pavement Testing*. Publication No. FHWA/IN/JTRP-2008/14, SPR-2419.

Nishiyama, T., Bhatti, M.A., and Lee, H.D. (2003). "Development of 3-D Finite Element Model to Quantify Bond Level of Thin Concrete Overlay" Transportation Research Board Annual Meeting, Washington, DC. CD-ROM. Paper Number: 03-2985.

Nishiyama, T., Lee, H.D., and Bhatti, M.A. (2005) "Investigation of Bonding Condition in Concrete Overlay by Laboratory Testing, Finite Element Modeling, and Field." *Transportation Research Record: Journal of the Transportation Research Board*, No. 1933, pp. 15–23. Transportation Research Board of the National Academies, Washington, D.C

Rasmussen, A.O., McCullough, B.F., Ruiz, J.M., Mack, J. and Sherwood, J.A. (2002). "Identification of Pavement Failure Mechanisms at FHWA Accelerated Loading Facility Ultrathin Whitetopping Project." *Transportation Research Record: Journal of the Transportation Research Board*, No. 1816, pp. 148-155. Transportation Research Board of the National Academics, Washington, DC

Rasmussen, R.O. and Rozycki, D.K. (2004). *Thin and Ultra-Thin Whitetopping*. NCHRP Synthesis of Highway Practice 338, National Cooperative Highway Research Program, National Research Council, Washington, D.C.

Roesler, J., Bordelon, A., Ioannides, A., Beyer, M., and Wang, D. (2008). *Design and Concrete Material Requirements for Ultra-Thin Whitetopping*. Publication FHWA-ICT-08-016. Illinois Center for Transportation, IL.

Roesler, J.R., Cervantes, V.G. and Amirkhanian, A.N. (2012). "Accelerated Performance Testing of Concrete Pavement with Short Slabs." *International Journal of Pavement Engineering*. 13 (6), 494-507.

Sheehan, M.J., Tarr, S.M., Tayabji, S. (2004). *Instrumentation and Field Testing of Thin Whitetopping Pavement in Colorado and Revision of the Existing Colorado Thin Whitetopping Procedure*. Report No. CDOT-DTD-R-2004-12. Colorado Department of Transportation.

Tarr, S. M., Sheehan. M.J., and Okamoto, P.A. (1998) *Guidelines for the Thickness Design of Bonded Whitetopping Pavement in the State of Colorado*. Report No. CDOTDTD- R-98-10, Colorado. Department of Transportation, Denver, CO.

Wu, C.L., Tarr, S.M., Refai, T.M., Nagai, M.A., and Sheehan, M.J. (1998). *Development of Ultra-Thin Whitetopping Design Procedure*. Report RD 2124. Portland Cement Association, Skokie, IL.

Vandenbossche, J. M. and Fagerness, A.J. (2002) "Performance, Analysis, and Repair of Ultra-thin and Thin Whitetopping at Minnesota Road Research Facility." *Transportation Research Record: Journal of Transportation Research Board*, No. 1809, pp. 191-198, Transportation Research Board of the National Academics, Washington, DC.

Vandenbossche, J.M., Dufalla, N. and Li, Z. (2013). *A Revised Thin and Ultra-Thin Bonded Whitetopping Design Procedure*. Transportation Research Record: Journal of Transportation Research Board, Transportation Research Board of the National Academics, Washington, DC. In press.